Evidence for Plasma Heating at Thin Current Sheets in the Solar Wind

Zilu Zhou[1,2] , Xiaojun Xu[1,2] , Pingbing Zuo[3] , Yi Wang[3], Qi Xu[3], Yudong Ye[1,2], Jing Wang[1,2,4] , Ming Wang[1,2,5] ,
Qing Chang[1,2] , Xing Wang[1,2], and Lei Luo[1,2]

[1] State Key Laboratory of Lunar and Planetary Sciences, Macau University of Science and Technology, Macau, People's Republic of China; xjxu@must.edu.mo
[2] CNSA Macau Center for Space Exploration and Science, Macau, People's Republic of China
[3] Institute of Space Science and Applied Technology, Harbin Institute of Technology, Shenzhen 518000, People's Republic of China
[4] Planetary Environmental and Astrobiological Research Laboratory (PEARL), School of Atmospheric Sciences, Sun Yat-sen University, Zhuhai 519000, People's Republic of China
[5] Institute of Space Weather, Nanjing University of Information Science and Technology, Nanjing 210044, People's Republic of China

Abstract

Plasma heating at thin current sheets in the solar wind is examined using magnetic field and plasma data obtained by the WIND spacecraft in the past 17 years from 2004 to 2019. In this study, a thin current sheet is defined by an abrupt rotation (larger than $45°$) of the magnetic field direction in 3 s. A total of 57,814 current sheets have been identified, among which 25,018 current sheets are located in the slow wind and 19,842 current sheets are located in the fast wind. Significant plasma heating is found at current sheets in both slow and fast wind. Proton temperature increases more significantly at current sheets in the fast wind than in the slow wind, while the enhancement in electron temperature is less remarkable at current sheets in the fast wind. The results reveal that plasma heating commonly exists at thin current sheets in the solar wind regardless of the wind speed, but the underlying heating mechanisms might be different.

Unified Astronomy Thesaurus concepts: Solar wind (1534); Interplanetary turbulence (830)

1. Introduction

Current sheets are ubiquitous in interplanetary space. These structures used to be classified as classical discontinuities, that is, boundaries separating plasmas with dramatically different properties (tangential discontinuities, TDs) or steepened Alfvén waves (rotational discontinuities, RDs; Burlaga 1968; Hudson 1970; Tsurutani & Smith 1979; Tsurutani et al. 2002; Borovsky 2008). Recent studies indicate that thin current sheets are associated with intermittent structures generated by turbulence (Vasquez et al. 2007; Greco et al. 2008, 2009; Zhang et al. 2015; Yang et al. 2017). High-resolution data obtained in the turbulent magnetosheath of Earth revealed that local dissipation of magnetic energy leading to plasma heating could take place at such small-scale intermittent structures (Chasapis et al. 2015, 2017, 2018; Chhiber et al. 2018). The intermittent structures generated by turbulence are suggested to be candidates for reconnection sites in simulations (Servidio et al. 2009, 2015). This is consistent with observational studies in Earth's magnetosheath, revealing that magnetic reconnection in thin current sheets can facilitate the dissipation of magnetic energy at kinetic scales to accelerate and heat plasmas (Retinò et al. 2007; Sundkvist et al. 2007; Phan et al. 2018; Stawarz et al. 2019).

It has also long been conjectured that strong current sheets in the solar wind are sites of enhanced dissipation and plasma heating (Burlaga 1968; Leamon et al. 2000). Due to the low time resolutions of solar wind plasma measurements, very few current sheets with Hall effects indicating ongoing magnetic reconnection have been directly observed in the solar wind (Xu et al. 2015; Mistry et al. 2016), but reconnection exhausts bounded by bifurcated current sheets are prevalently encountered (Gosling 2012). A statistical study carried out by Osman et al. (2011) using solar wind data obtained by the ACE spacecraft showed that intermittent structures were associated with elevated proton temperature, indicating that inhomogeneous heating linked to current sheets occurs in the solar wind. By contrast, Borovsky & Denton (2011) selected over 100,000 strong current sheets and found no evidence for local enhancement of proton and/or electron temperature in the vicinity of the current sheets. The statistical association of current sheets with temperature increase was interpreted as more current sheets being counted in the fast solar wind. Fast wind is typically less dense but hotter than slow wind. Moreover, the magnetic field in fast wind fluctuates much more than in slow wind, unraveling the presence of strong Alfvénic fluctuations (Bruno & Carbone 2013). This conflict was partly solved by Osman et al. (2012) who performed a superposed-epoch analysis on proton temperature around strong current sheets, finding significant local enhancement (with a width of 1000 ion inertial lengths) around the strong current sheets. Nevertheless, whether a local dissipation process occurs at current sheets in the fast solar wind remains unknown. Moreover, if magnetic reconnection plays an important role in the plasma heating, the heating range should be localized around thin current sheets with a thickness of a few ion inertial lengths. A statistical study of current sheets in the magnetic cloud sheath regions show that significant localized heating only occurs at thin current sheets with a width of several ion inertial lengths (Zhou et al. 2019). Such localized proton heating effect at thin current sheets also occurs in the younger solar wind observed by Parker Solar Probe (Qudsi et al. 2020).

In this Letter, we will check whether local heating exists at thin current sheets in the solar wind at 1 au, and if exists, whether the heating profile differs between current sheets in the slow and fast winds.

2. Data and Events

Solar wind data from 2004 June 1 to 2019 December 31, measured by the WIND spacecraft at L1 point are used to analyze the current sheets. The magnetic field and plasma data used to analyze the associated local heating of current sheets are obtained from the Magnetic Field Investigation (MFI, Lepping et al. 1995) and the Three Dimensional Plasma analyzer (3DP, Lin et al. 1995) on board the WIND spacecraft, respectively. The time resolutions are both 3 s.

Several automated methods have been applied to identify current sheets in the solar wind, either considering directional changes of magnetic field only or jointly with strength changes (Li 2007; Greco et al. 2008; Zhdankin et al. 2013). In this work, thin current sheets in the solar wind are defined by directional changes $\Delta\theta > 45°$ of the magnetic field over a 3 s time interval, where $\Delta\theta = \cos^{-1}(\boldsymbol{B}(t + 3) \cdot \boldsymbol{B}(t)/(|\boldsymbol{B}(t)||\boldsymbol{B}(t + 3)|))$. A total of 57814 thin current sheets with valid plasma data are identified. The current sheets are categorized according to the ambient solar wind speed V_{sw}, which is the averaged proton speed over an 1 hr interval centered at each current sheet. 25018 current sheets are located in slow wind ($V_{\mathrm{sw}} \leqslant 450\,\mathrm{km\,s}^{-1}$), while 12954 current sheets are located in fast wind ($V_{\mathrm{sw}} \geqslant 600\,\mathrm{km\,s}^{-1}$). The remaining 20202 current sheets are located in the solar wind with speed in the range from 450 kms^{-1} to 600 kms^{-1}.

3. Results

Figure 1 shows the distributions of the ratios of the proton and electron temperatures at the location of a thin current sheet to the temperatures in the adjacent plasmas. For a current sheet identified at time t_i, the temperature inside the sheet is calculated as the average of the temperature measured at the leading edge and the trailing edge, i.e., $0.5(T_{t_i} + T_{t_{i+1}})$. The ratios are calculated as $(T_{t_i-\Delta t} + T_{t_{i+1}+\Delta t})/(T_{t_i} + T_{t_{i+1}})$, where Δt are 3, 30, and 60 s for the green, blue, and red curves, respectively. The dashed vertical lines denote the corresponding median number of each data set.

Figure 1(a) shows the distributions of the ratios of the proton temperature at the location of a thin current sheet to the proton temperature in the adjacent plasmas. The median numbers are 1.007, 1.028, 1.036 for the green, blue, and red curves, respectively. This indicates that protons at thin current sheets are significantly hotter than surrounding protons for more than a half of the identified current sheets.

Figure 1(b) shows the distributions of the ratios of the electron temperature at the location of a thin current sheet to the electron temperature in the adjacent plasmas. The median numbers are 1.003, 1.009, 1.011 for the green, blue, and red curves, respectively. This indicates that electrons at thin current sheets are also obviously hotter than surrounding electrons for more than half of the identified current sheets, although the observed enhancement is not as significant as the increase in proton temperature.

The reason for the statistical association of current sheets with temperature increase, interpreted by Borovsky & Denton (2011), is that the hotter fast wind contains more strong current sheets. Indeed, thin current sheets are more prevalent in the fast wind. This can be seen from the comparable counts for the current sheets identified (25018 in the slow wind and 12954 in the fast wind) despite that fast wind streams are rarely observed in the ecliptic plane at 1 au compared to the slow wind. However, remarkable proton heating exists in the fast wind, as demonstrated in Figure 2. Figure 2 shows the median numbers of the ratios of proton and electron temperatures at different distance from the leading edges of current sheets to the proton/electron temperature at the leading edge of the current sheets, $T(\Delta r)/T_{\mathrm{cs}}$ in the slow wind (blue lines) and fast wind (red lines), respectively. The distance Δr is normalized by ion inertial length (d_i) for each current sheet crossings, calculated as $\Delta r = V_{\mathrm{sw}}\Delta t/d_i$.

As shown in Figure 2(a), the proton temperature ratios drop abruptly to 96% within 300 d_i for both data sets of current sheets in the fast and slow winds. Then the ratios drop gradually to about 94% in the fast wind and 93% in the slow wind at a distance of 2000 d_i. Note that the dimensionless temperature ratio is used here. This indicates significant proton heating occurs in the vicinity of the thin current sheets regardless of the proton temperature of the ambient wind. Considering the fast wind is usually hotter than the slow wind, temperature enhancements at thin current sheets are more remarkable than current sheets in the slow wind, as we will also see in Figure 3.

Figure 2(b) presents the median numbers of the ratios of electron temperatures at different distance from the leading edges of current sheets to the electron temperature at the leading edges of the current sheets. A slight increase (about 1%) within 100 d_i from the current sheets can be found at the center, and then the ratios remain unchanged in the fast wind. In the slow wind, the electron temperature ratios drop quickly to 98.5% within 200 d_i, and then decrease gradually to about 98% at a distance of 2000 d_i. This indicates that electron heating is not as significant as proton heating, especially for the current sheets in the fast solar wind.

Figure 3 shows the results of a superposed-epoch analysis of magnetic field and selected plasma parameters for the identified current sheets. The scalar quantity obtained by superposed-epoch analysis is calculated as $Q = \langle Q(t_i + \Delta t)\rangle$, where Q refers to the corresponding parameter in each panel, t_i is the time at the leadng edge of each identified current sheet, and Δt is the time difference relative to t_i.

Figures 3(a) and (b) show the averaged proton temperatures in the vicinity of the thin current sheets in the fast (in red) and slow solar winds (in blue), respectively. The elevation of proton temperature at current sheets in the fast wind is more significant ($\Delta T_p \approx 20{,}000 K$) than that in the slow wind ($\Delta T_p \approx 8000 K$). Figures 3(c) and (d) show the averaged electron temperatures in the vicinity of the thin current sheets in the fast (in red) and slow solar winds (in blue), respectively. The observed electron temperature enhancement is less than the proton temperature enhancement. The increase of electron temperature at current sheets in the fast wind is smaller ($\Delta T_e \approx 1000 K$) than that in the slow wind ($\Delta T_e \approx 1500 K$). Magnetic field strength decreases at current sheets, as shown in Figure 3(e).The decreases of the magnetic field magnitude are comparable at current sheets in the fast wind and slow wind. However, since the magnetic field of current sheets in the fast wind is stronger than that in the slow wind, the loss of magnetic field energy is greater at current sheets in the fast wind, as shown in Figure 3(f). Figure 3(g) shows that magnetic field increment at current sheets in the fast wind is much larger, indicating stronger intermittency in the fast wind.
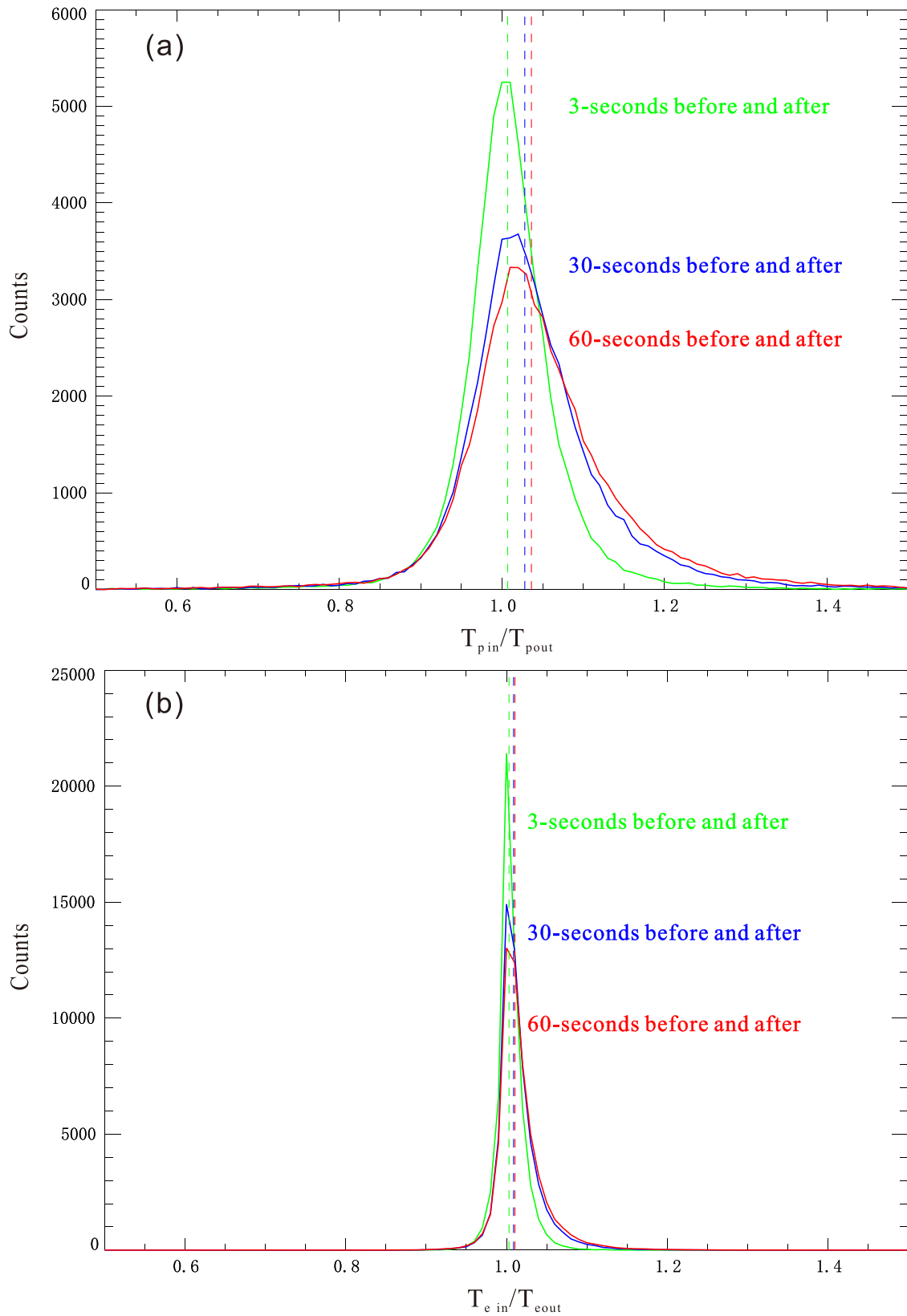
Figure 1. Occurrence distributions: (a) the ratios of the proton temperatures at current sheets to those outside current sheets, and (b) the ratios of the electron temperatures at current sheets to those outside current sheets. The dashed vertical lines denote the corresponding median number of each data set.

4. Summary and Discussion

Plasma heating at thin current sheets in the solar wind is examined using magnetic field and plasma data obtained by the WIND spacecraft over the past 17 years from 2004 to 2019. A total of 57,814 thin current sheets at a spatial scale of several ion inertial lengths have been identified, among which 25,018
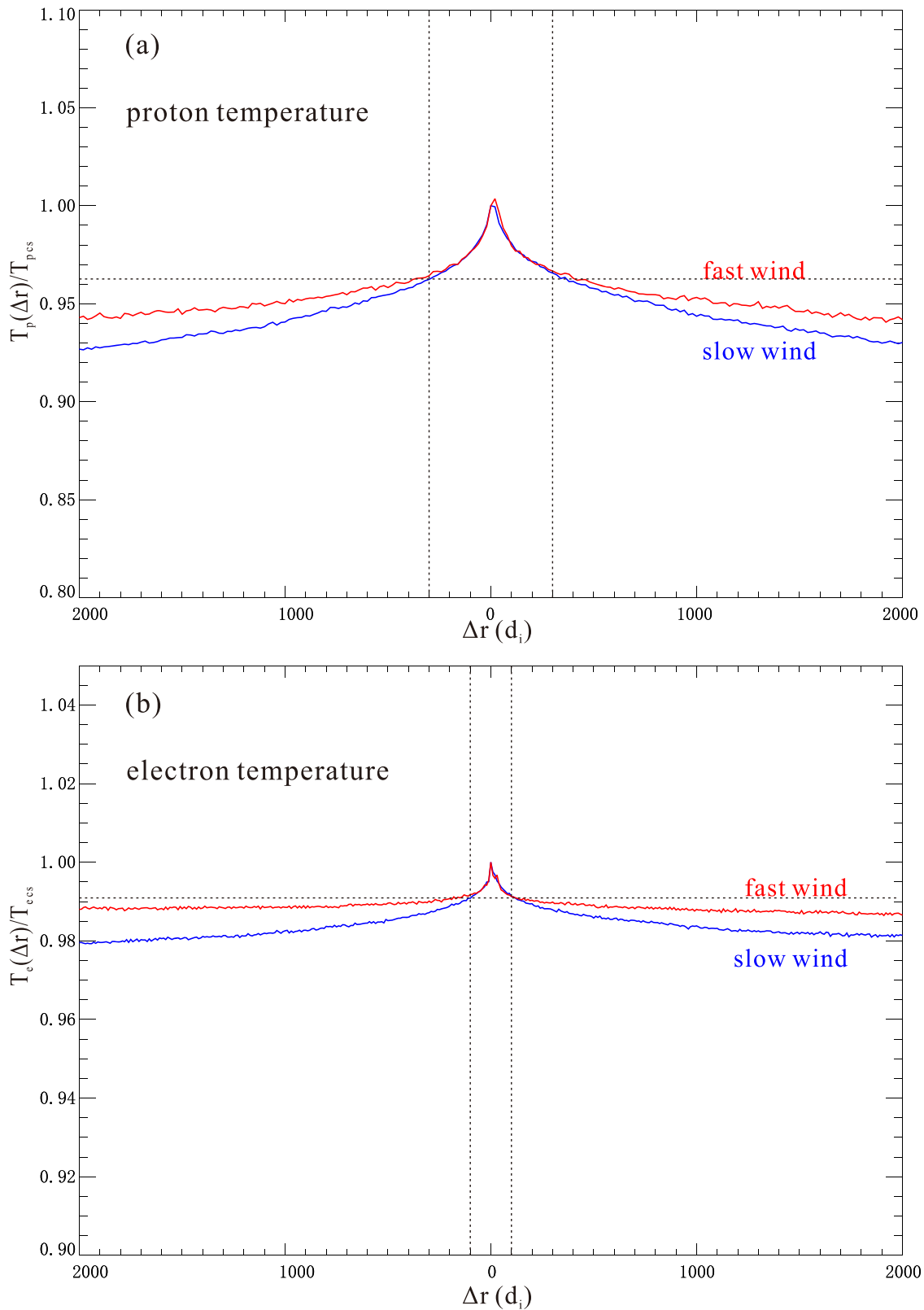
Figure 2. Median numbers of the ratios of (a) proton temperature and (b) electron temperature at different distance from the leading edge of current sheets to the proton/electron temperature at the leading edge of the current sheets in the slow wind (blue lines) and fast wind (red lines), respectively.

current sheets are located in the slow wind and 19,842 current sheets are located in the fast wind. Significant elevation of plasma temperatures can be found in the vicinity of the thin current sheets regardless of the wind speed. Our result supports the conjecture that thin current sheets could be sites of local heating in the solar wind. Nevertheless, the heating profile differs between current sheets in the slow and fast winds. For current sheets in the fast wind, the elevation of proton
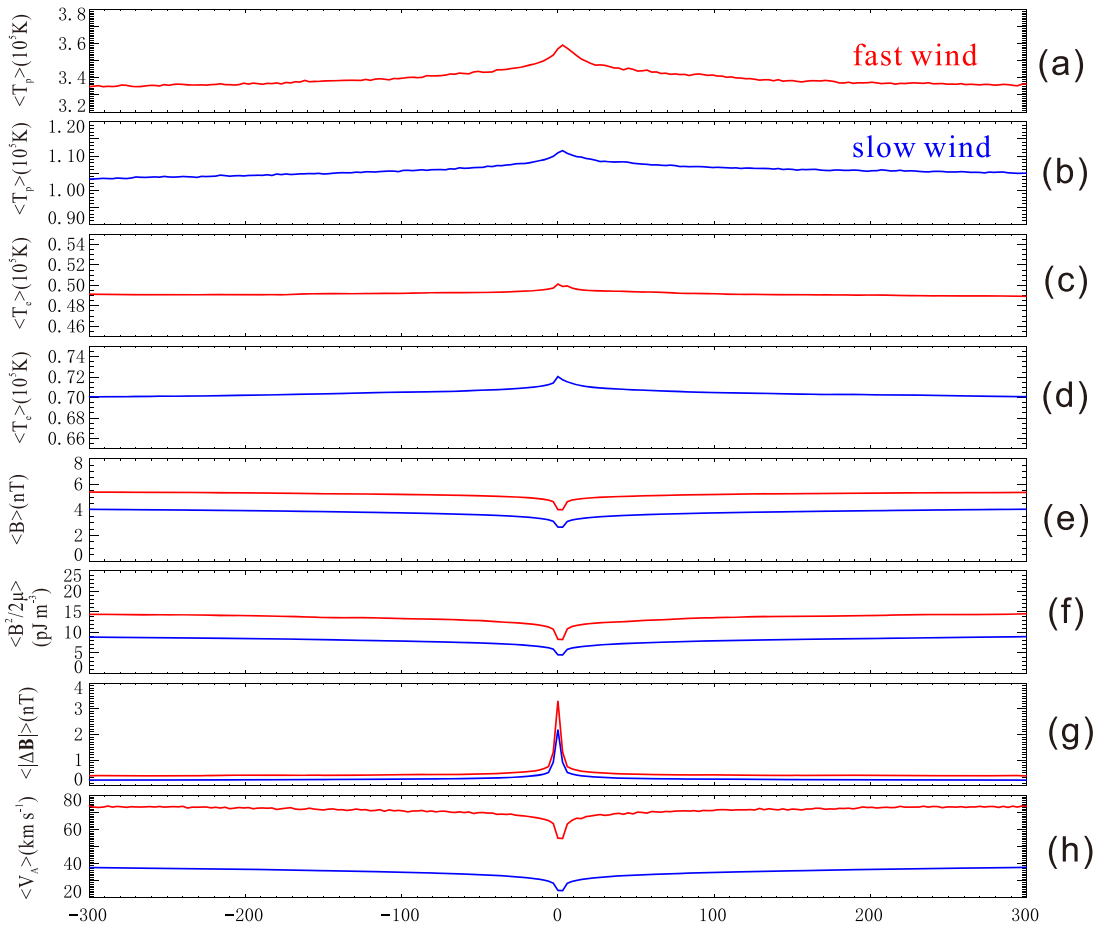
Figure 3. Superposed-epoch analysis of identified thin current sheets in fast wind (red lines) and slow wind (blue lines): (a) proton temperature in fast wind, (b) proton temperature in slow wind, (c) electron temperature in fast wind, (d) electron temperature in slow wind, (e) magnetic field intensity, (f) magnetic energy density, (g) magnetic field increment, and (h) Alfvén speed.

temperature is more significant but electrons are less heated compared to those of current sheets in the slow wind. This difference indicates the underlying heating mechanism might be different for current sheets in the slow wind and fast wind.

It has been suggested that current sheets could be natural sites for magnetic reconnection (Servidio et al. 2009; Osman et al. 2014). Hence, magnetic reconnection is considered to be an effective way to heat the plasma around current sheets (Osman et al. 2011, 2012). Studies of plasma heating through magnetic reconnection at Earth's magnetopause reveal that the elevations of proton and electron temperatures are both correlated with the inflow Alfvén speed (Phan et al. 2013, 2014). The ratio of ion to electron heating ($\Delta T_p/\Delta T_e$) in magnetopause exhausts is 7.6 on average. In our study, the ratio for current sheets in the slow wind is 5, which is consistent with the results in Phan et al. (2014). This indicates that magnetic reconnetion may be an important dissipation mechanism in the local heating at current sheets in the slow wind. However, the ratio of ion to electron heating for current sheets in the fast wind is 20, which is much larger than that in the reconnection exhausts. The averaged elevation of electron temperature at current sheets in the fast wind is smaller than that at current sheets in the slow wind, despite that the background Alfvén speed is larger in the fast wind, as shown in Figure 3(h). That means, for a large amount of current sheets in the fast wind, protons are heated while significant electron heating has not been observed beyond ion scales. Note that the

occurrence rate of magnetic reconnection observed at 1 au is lower in the fast wind (Gosling 2012). Therefore, magnetic reconnection may not dominate the plasma heating solely at current sheets in the fast wind. Other possible dissipation mechanisms at thin current sheets in the fast solar wind need to be further studied.

ORCID iDs

Zilu Zhou ⓘ https://orcid.org/0000-0002-4463-8407
Xiaojun Xu ⓘ https://orcid.org/0000-0002-2309-0649
Pingbing Zuo ⓘ https://orcid.org/0000-0003-4711-0306
Jing Wang ⓘ https://orcid.org/0000-0003-0471-5532
Ming Wang ⓘ https://orcid.org/0000-0002-3290-8721

Qing Chang ⓘ https://orcid.org/0000-0003-4883-949X

References

Borovsky, J. E. 2008, JGRA, 113, A08110
Borovsky, J. E., & Denton, M. H. 2011, ApJL, 739, L61
Bruno, R., & Carbone, V. 2013, LRSP, 10, 2
Burlaga, L. F. 1968, SoPh, 4, 67
Chasapis, A., Matthaeus, W. H., Parashar, T. N., et al. 2017, ApJ, 836, 247
Chasapis, A., Matthaeus, W. H., Parashar, T. N., et al. 2018, ApJL, 856, L19
Chasapis, A., Retinò, A., Sahraoui, F., et al. 2015, ApJL, 804, L1
Chhiber, R., Chasapis, A., Bandyopadhyay, R., et al. 2018, JGRA, 123, 9941
Gosling, J. T. 2012, SSRv, 172, 187
Greco, A., Chuychai, P., Matthaeus, W. H., Servidio, S., & Dmitruk, P. 2008, GeoRL, 35, L19111
Greco, A., Matthaeus, W. H., Servidio, S., Chuychai, P., & Dmitruk, P. 2009, ApJL, 691, L111
Hudson, P. D. 1970, P&SS, 18, 1611
Leamon, R. J., Matthaeus, W. H., Smith, C. W., et al. 2000, ApJ, 537, 1054
Lepping, R. P., Acũna, M. H., Burlaga, L. F., et al. 1995, SSRv, 71, 207
Li, G. 2007, ApJL, 672, L65
Lin, R. P., Anderson, K. A., Ashford, S., et al. 1995, SSRv, 71, 125
Mistry, R., Eastwood, J., Haggerty, C., et al. 2016, PhRvL, 117, 185102
Osman, K. T., Matthaeus, W. H., Gosling, J. T., et al. 2014, PhRvL, 112, 215002
Osman, K. T., Matthaeus, W. H., Greco, A., & Servidio, S. 2011, ApJL, 727, L11
Osman, K. T., Matthaeus, W. H., Wan, M., & Rappazzo, A. F. 2012, PhRvL, 108, 261102
Phan, T. D., Drake, J. F., Shay, M. A., et al. 2014, GeoRL, 41, 7002
Phan, T. D., Eastwood, J. P., Shay, M. A., et al. 2018, Natur, 557, 202
Phan, T. D., Shay, M. A., Gosling, J. T., et al. 2013, GeoRL, 40, 4475
Qudsi, R. A., Maruca, B. A., Matthaeus, W. H., et al. 2020, ApJS, 246, 46
Retinò, A., Sundkvist, D., Vaivads, A., et al. 2007, NatPh, 3, 236
Servidio, S., Matthaeus, W. H., Shay, M. A., Cassak, P. A., & Dmitruk, P. 2009, PhRvL, 102, 115003
Servidio, S., Valentini, F., Perrone, D., et al. 2015, JPlPh, 81, 325810107
Stawarz, J. E., Eastwood, J. P., Phan, T. D., et al. 2019, ApJL, 877, L37
Sundkvist, D., Retinò, A., Vaivads, A., & Bale, S. D. 2007, PhRvL, 99, 025004
Tsurutani, B. T., Galvan, C., Arballo, J. K., et al. 2002, GeoRL, 29, 1528
Tsurutani, B. T., & Smith, E. J. 1979, JGR, 84, 2773
Vasquez, B. J., Abramenko, V. I., Haggerty, D. K., & Smith, C. W. 2007, JGR, 112, A11102
Xu, X., Wang, Y., Wei, F., et al. 2015, NatSR, 5, 8080
Yang, L., Zhang, L., He, J., et al. 2017, ApJ, 851, 121
Zhang, L., He, J., Tu, C., et al. 2015, ApJL, 804, L43
Zhdankin, V., Uzdensky, D. A., Perez, J. C., & Boldyrev, S. 2013, ApJ, 771, 124
Zhou, Z., Zuo, P., Wei, F., et al. 2019, ApJL, 885, L13